# Soft Gold Nanowire Sponges for Strain-insensitive Conductors, Wearable Energy Storage and Catalytic Converters

*Fenge Lin[a,b], Kaixuan Wang [a,b], Tiance An [a,b], Bowen Zhu [a,b], Yunzhi Ling [a,b], Shu Gong [a,b], Siyuan Liu [a,b] and Wenlong Cheng [a,b,*]*

[a] *Department of Chemical Engineering, Monash University, Clayton, 3800 Victoria, Australia*

[b] *The Melbourne Centre for Nanofabrication, Clayton, 3168 Victoria, Australia*

**Corresponding author: Wenlong.Cheng@monash.edu*

*† Electronic supplementary information (ESI) available. See DOI: (will be filled in by the editorial staff)*

## Abstract

Electronics is evolving from rigid, flexible to ultimate stretchable electronics in which active optoelectronic materials are required to deposit onto or embedded into elastomeric materials. We have recently demonstrated a powerful solution-based electroless gold coating technology, which enables growth of enokitake-like gold nanowires on two-dimensional elastomeric sheets and one-dimensional fibers for a wide of applications in wearable bioelectronics. Here, we show that such an elastomeric gold coating technology can be extended to three-dimensional (3D) elastomeric sponges. We have successfully grown vertically-aligned enokitake-like gold nanowires (v-AuNWs) uniformly throughout 3D sponge skeletons, leading to highly conductive sponge with a conductivity up to about 1500 S/m. This, in conjunction with embedment of Ecoflex into porous v-AuNWs sponge, leads to a strain-insensitive conductor that only changes about 17.3% in resistance under 50% strain, 83.3% in resistance under 100% strain. The conductor can be stretched up to ~340% strain before losing conductivity. Furthermore, the strain-insensitive sponge conductors are used as electrodes to fabricate elastic supercapacitor which can retain 102% and 99% of initial capacitance under 50% compression strain and 180$^{o}$ bending, respectively. In addition, our gold sponge is also catalytically active and can serve as recyclable 3D porous catalyst (achieving 90% conversion efficiency even after 10 cycles of 4-nitrophenol reduction reaction). The results presented here demonstrate a simple yet efficient wet chemical approach to multifunctional sponge for applications in stretchable electronics, wearable energy devices and catalysis.

## Introduction

Intelligent biological system is mainly made from soft materials including key building blocks of DNA, RNA, protein and polysaccharide. To render the state-of-the-art electronics more intelligent, researchers are attempting to deposit or embed optoelectronic materials into/onto elastomeric materials.[1, 2] In this context, 2D elastomeric sheets and 1D elastomeric fibers have been widely used as substrates for integrating with active materials such as carbon, metal, silicon and conducting polymers for developing various soft electronic systems.[3-10] In addition, elastomeric sponges, such as polyurethane sponge (PU sponge), have also been exploited in soft electronics,[11-13] in which 3D porous frameworks, light-weightness, mechanical elasticity can be combined with electrical conductivity leading to novel sensors and energy devices.[14-18]

The dip-coating approach represents the dominant strategy to fabricate conductive sponge due to its simplicity. With this approach, conductive ink, such as CNT,[14, 16, 19] carbon black,[20] graphene,[21, 22] silver nanowires[12, 23] have been successfully used for constructing conductive sponges. In addition, freeze-drying represents another strategy to fabricate conductive sponges. For example, copper nanowire aerogels[11, 24] have been successfully obtained by mixing PVA and copper nanowire solution followed by freeze-drying. Conductive aerogel sponges have been achieved by directly freeze-drying suspensions of silver nanowire,[25] graphene,[26] and CNT-rGO[27]. In addition, polymer-assisted copper deposition[13] and gold ion sputter-based metallic sponges[15] have also been reported in the literature. Despite these encouraging advances, some challenging issues remain. The dip-coating approach typically suffers from poor adhesion between conductive fillers and sponge skeleton; carbon-based sponge sometimes only offers low conductivity; ion-sputtered metallic film may experience crack under mechanical deformation.

Here, we report on a direct conformal electroless gold-coating strategy to grow highly conductive gold nanowire films uniformly throughout PU sponge skeletons. In our recent reports, we have described a facile yet powerful gold nanowire coating technology on various 2D planar elastomeric

sheets[9] and 1D elastomeric fibers,[7] which have demonstrated exciting applications in skin-like wearable sensors[28, 29] and energy devices.[30-32] Unlike conventional gold-coating technology fabricated by evaporation or electrodeposition, our gold film possesses enokitake-like Janus morphologies, leading to unconventional optical, wetting, electrical, electrochemical and mechanical properties depending on which sides exposed.[33, 34] In this work, we show this gold nanowire coating technology could be extended to 3D sponge skeleton achieving uniform conformal coating with a conductivity of up to about 1500 S/m. Further embedding gold sponge into Ecoflex led to a high-performance strain-insensitive stretchable conductor that only changes 17.3% in resistance under 50% strain, 83.3% in resistance under 100% strain. This strain-insensitive property in conjunction with high conductivity and porous structure, motivated us to design a stretchable supercapacitor with a capacitance of 127.3 mF $cm^{-3}$ showing negligible performance deterioration even under 50% compression strain and 180° bending angles. Interestingly, we found that our gold sponge could efficiently catalyse 4-nitrophenol into 4-aminophenol under ambient conditions with 90% efficiency even after 10 reaction cycles. Our results indicate that this gold nanowire sponge is multifunctional soft materials platform for future sensing and energy applications.

## Results and Discussion

**Figure 1**A illustrates the gold nanowire sponge preparation process. Firstly, bare sponge was treated by air plasma to render its surface hydrophilic, which was followed by the amine modification by using (3-aminopropyl)trimethoxysilane (APTMS) in a hydrolysis reaction. Then the amine-functionalized sponge was immersed into a gold seeds solution for 2 h. This step led to the attachment of gold seeds onto the PU sponge skeleton based on electrostatic attractions. Further immersion of gold seed-decorated sponge into a growth solution containing gold precursors (Gold (III) chloride trihydrate), surfactants (4-Mercaptobenzoic acid) and reducing agent (L-ascorbic acid), enable growth of enokitake-like vertically aligned gold nanowires (v-AuNWs) perpendicular to PU surface.

**Figure 1**B and C are the optical images of PU sponge before and after v-AuNWs growth, respectively. Evidently, the gold coating changed the optical appearance from light yellow to brown. Nevertheless, the deposition of v-AuNWs did not alter mechanical properties of PU sponge. The gold sponge retained excellent elastic property and could bear folding (**Figure 1**D) and compressing (**Figure S1**A). The further stress-strain characterization of PU sponge and v-AuNWs sponge demonstrated their similar mechanical properties. Both strain-stress curves displayed three different regions in the loading process (**Figure S1**B). The stress increases linearly with the strain under about 5% which is in the elastic region. This is followed by the plateau region up to about 50% strain, in which the absorbed energy dissipated significantly. With further strain, the system entered into the densification region, in which the stress increased rapidly with strains because of the significant pore volume decrease. Hysteresis loops appear in the unloading process due to dissipation of mechanical energy, in good agreement with the reported literature.[16]

Scanning electron microscope (SEM) was used to characterize some the as-synthesized v-AuNWs foam (**Figure 1**E and **Figure S2**). In general, the v-AuNWs gold film was continuous attached onto the sponge skeleton without evident cracks observed. Nevertheless, enokitake-like nanowires could be observed in some defective areas as shown **Figure 1**F and G and supporting **Figure S**3). The results are consistent with our previous study, in which the gold nanowires stood perpendicularly to the supporting surfaces with nanoparticle side exposed, and nanowire side attached to the substrates[33]. Our previous study[9] shows that the length of AuNWs is highly dependent on the types of substrates and the growth time. For the PU foam in this work, we couldn't obtain very long nanowires possibly due to limited diffusion of growth solution into 3D porous matrix, unlike the case of planar substrate such as silicon surface. Nevertheless, we could still get long AuNWs by increasing the growth time, achieving a length of ~2 μm (**Figure S4**). This gold sponge with an estimated conductivity of ~1500 S/m (**Figure S6**) based on effective cross-sectional area of skeleton (**Figure S5**). In addition, the v-AuNWs had excellent adhesion with sponge skeleton. They could survive in the normal Scotch tape test without stripped off v-AuNWs films (supporting **video S1**). The strong adhesion may be due to

the use of APTMS, which serves as a bifunctional molecular glue. Its amine side strongly interacts with v-AuNWs, and its silane sides covalently bond to PU sponge surfaces.

Because of uniform and conformal v-AuNWs coating throughout PU skeleton, the gold sponge could exhibit the sufficiently high conductivity to be used as electrodes for applications in soft electronics. With their further embedment into Ecoflex, we could obtain strain-insensitive conductor. By establishing reliable contact with the v-AuNWs sponge at both ends before embedment with Ecoflex, we found that the Ecoflex embedment did not affect the conductivity of the gold sponge as demonstrated by the overlapping I-V curves (**Figure 2**A). As shown in **Figure 2**B, the resistance change ($R/R_0$) is about 1.26 under 60% strain and 1.83 under 100% strain for a particular sample. Under 100% strain, the resistance value is about 32.5 Ω (**Figure S7**A). In addition, we tested resistance of five samples and the average $R/R_0$ value under 100% strain is about 2.15 (**Figure S7**B). For a typical sample, when the applied strain was less than 50%, all the I-V curves overlapped (**Figure 2**C), and when the strain over 60%, the current dropped gradually. With the increased strain to 100%, the current continued to drop about 28% (**Figure S7**C). With further increased strain to 340%, the v-AuNWs sponge became non-conductive (**Figure 2**B). Such a high stretchability limit wasn't reported in the elastomer-embedded sponge based conductors reported in literature[12,13]. As expected, v-AuNWs film may crack with the extent depending on local strain level. The morphological features of v-AuNWs sponges/Ecoflex composites at some domains were therefore characterized by SEM (**Figure S8**). Under strains, the porous sponge skeleton elongated in the strain directions (**Figure S8**A, B and C). Cracks were evident on the branch of sponge skeleton, especially distributed on the branch along with the strain direction (**Figure S8** b2 and c2). The junction areas usually show much less significant cracks than the branch skeleton areas (**Figure S8** b1 and c1). Our strain-insensitive conductors are highly durable with negligible changes in conductivities under the 5000 stretch-release cycles at 30% strain (**Figure 2**D). There is slight increase of $R/R_0$ after 5000 cycles, which can be explained by SEM images (**Figure S10**), the v-AuNWs film showed cracks in the branch of the sponge skeleton after 5000 stretching cycles. After 5000 stretching cycles, the v-AuNWs

sponge/Ecoflex composites could pass the tape test with no materials peeled off as shown in supporting **video S2**. As a practical demonstration of our strain-insensitive conductors, we show that a LED maintained stable light intensity even under 200% strain as shown in **Figure S11** (see more details shown in the attached **video S3**).

Without Ecoflex embedment, our gold sponge also showed excellent strain-insensitive conductivity, which motivated us to design soft and flexible supercapacitors. Typically, the resistance decreased with compression strain increased and almost remain stable to bending (**Figure S12**). Compression could also cause cracks on the gold sponge, but they distributed unevenly and appeared to dominate the areas next to PU skeleton junction (**Figure S13**). Upon the compression load removal, most of the cracks were gone (**Figure S14**). Moreover, the v-AuNWs sponges had an estimated porosity of 50.3±2.4% (**Figure S5**) with interconnected pores, ensuring facile access of electrolytes to porous 3D v-AuNW surfaces. To enhance the capacitance, we deposited a layer of pseudocapacitive polyaniline (PANI) on v-AuNWs sponge skeleton by electrodeposition. This led to slightly rougher surface of gold sponge (**Figure S15**). Based on PANI/v-AuNWs sponge, we assembled the soft and compressible supercapacitors (**Figure 3**A). Sputtered Au films on poly(ethyleneterephthalate) (PET) substrates were used as current collectors. Filter paper served as a separator and the electrolyte was poly(vinyl alcohol)/$H_2SO_4$ (PVA/ $H_2SO_4$). Cyclic voltammetry (CV) and galvanostatic charge-discharge (GCD) tests were carried out with the voltage set between 0 and 0.8 V. As illustrated in **Figure 3**B, the CV curves maintain quasi-rectangular shapes with scan rate increased up to 1000 mV $s^{-1}$. The GCD curves (**Figure 3**C) are symmetric triangular shapes indicating reversible charge-discharge behaviour. The volumetric capacitance calculated from CV curves with different scan rates are summarized in **Figure 3**D. The v-AuNWs/PANI-based supercapacitor exhibited a volumetric capacitance of 127.3 mF $cm^{-3}$ at the scan rate of 10 mV $s^{-1}$(calculated from equation (3)), with a capacitance retention of 70.1% under 200 mV $s^{-1}$. Then we examined the stability of our supercapacitors under 2000 cycles of CV tests at 200 mV $s^{-1}$ (**Figure S16**), showing an 83% capacitance retention after 2000 cycles.

The as-prepared v-AuNWs/PANI sponge based supercapacitor could sustain extreme compressing and bending while maintaining its electrochemical performance. As shown in **Figure 3**E, when different compression strains up to 50% are applied to the supercapacitor, there are negligible deviation observed in the CV curves, indicating the excellent mechanical stability of the supercapacitors. The GCD curves shown in **Figure S17**A are consistent with CV curves. There was only very slight difference of capacitance observed under different compressible strains, with a capacitance retention of 102% under 50% compression strain (**Figure S17**B). In addition, our supercapacitor could retain about 93% of its original capacitance under repeated compression-release cycles for 1000 times at 50% strain (**Figure S17**C, D). The consistent results were obtained for the bending tests, where both CV curves (**Figure 3**F) and GCD curves (**Figure S18**A) almost kept unchanged even when the supercapacitor was bent from 0º to 180º. The capacitance retention is about 99% under 180°bending angle (**Figure S18**B). Even after 1000 bending cycles at the angle of 180º, our supercapacitor still showed a 94% capacitance retention (**Figure S18**C, D).

We further demonstrated stretchable supercapacitor by replacing paper separator with PVA/$H_2SO_4$ impregnated bare sponge as shown in **Figure S19**. This all-sponge-based supercapacitor could function at strained state with initial strain-insensitive capacitance at small strain level but increased capacitance at high strain level (**Figure S20**A). In particular, the capacitance increased significantly from 6.55 μF $cm^{-3}$ at no strain to 9.68 μF $cm^{-3}$ at 66% strain. This increase may be well interpreted by the "upzipping" of closely-spaced v-AuNWs under strains[33], enabling greater surface areas exposed electrolytes. Our all foam-based supercapacitor exhibited negligible capacitance changes under 180º bending and twisting (**Figure S20**B, C). Overall, our gold sponge-based supercapacitors exhibited better deformation-insensitive capacitance than the recent literatures with other materials (Table S1).

In addition to the aforementioned applications in soft electronics, the porous structure of sponge in conjunction with the vertically aligned gold nanowires could serve as 3D catalyst. The 3D structures offer high surface area and facile access to reactants. Simultaneously, it mimic the way that soft

artificial leave convert chemicals without the need of catalyst regeneration. As a model system, we investigated their catalytic property towards the reduction of 4-nitrophenol to 4-aminophenol with $NaBH_4$. As shown in **Figure 4**A, bare PU sponge and v-AuNWs sponge are immersed into the yellow mixed solution of 4-nitrophenol and $NaBH_4$ respectively for 20 min, the solution in contact with the v-AuNWs sponge turned colorless. In contrast, the solution contact with bare PU sponge still yellow after three days. The catalytic reaction progress was carefully monitored by UV-vis spectrometry. As demonstrated in **Figure 4**B, as the reaction time increased, the characteristic absorption peak of 4-nitrophenol at 400 nm decreased and simultaneously a new peak at 295 nm appeared and enhanced. This demonstrates the reduction of 4-nitrophenol to form 4-aminophenol. The catalytic reactions did not alter surface morphologies of v-AuNWs (**Figure S21**), which may be attributed to the strong adhesion of v-AuNWs to PU sponge skeleton and chemical inert nature of gold. One advantage of the v-AuNWs sponges for catalysis is that they could be reused simply by repeated immersion into a fresh mixed solution of 4-nitrophenol and $NaBH_4$. **Figure 4**C shows that the v-AuNWs sponge maintained the similar catalytic performance, with a slightly decrease (~10%) in the conversion efficiency after 10 reaction cycles. The reaction rate constant K could be estimated by the linear regression between $\ln(C_t/C_0)$ (where $C_t$ is the concentration of 4-nitrophenol at time t, wherein $C_t/C_0$ values of 4-nitrophenol were directly given by the relative intensity of the respective absorbance $A_t/A_0$) and reaction time (t) (**Figure 4**D). The estimated reaction constants for the first and tenth cycle are 0.167 $min^{-1}$ and 0.103 $min^{-1}$, respectively.

## Conclusion

In summary, we report a simple yet efficient gold nanowire coating technology to fabricate electrically conductive, mechanically soft, catalytically active gold sponges. Based on these features, we demonstrated their applications in strain-insensitive conductors, soft supercapacitors and catalytic conversion. In comparison to dip-coating, freeze-drying and ion-sputtering, our fabrication strategy simultaneously offers the advantages of conformal coating, robust gold/elastomer bonding interface and electroless deposition under ambient conditions. Therefore, we achieved a strain-insensitive

conductor; deformation-insensitive supercapacitor under straining, bending and twisting; and robust recyclable catalysis. We believe that our soft multifunctional v-AuNWs sponges may find a myriad of technical applications[35] in future intelligent system in which soft sensors and energy devices are required.

## Experimental Section

***Materials:*** Gold (III) chloride trihydrate ($HAuCl_4 \cdot 3H_2O$, 99.9%), sodium citrate tribasic dehydrate (99.0%), sodium borohydride ($NaBH_4$, 99.99%), (3-aminopropyl)trimethoxysilane (APTMS ), 4-mercaptobenzoic acid (MBA, 90%), L-ascorbic acid (L-AA), poly (vinyl alcohol) (PVA) powder, sulphuric acid ($H_2SO_4$), 4-nitrophenol (4-NP) and ethanol (analytical grade) were purchased from Sigma-Aldrich. All chemicals were used as received unless otherwise indicated. Kitchen sponge (with a density of 0.03 $g/cm^3$) was purchased from Coles, Australia. All solutions were prepared using deionized water (resistivity >18 $M\Omega\ cm^{-1}$). Conductive wires were purchased from Adafruit. Ecoflex (0030) was purchased from Smooth-on.

***Synthesis of enokitake-like vertically aligned gold nanowires sponge*:** A modified seed-mediated approach was used as our previous works.[9, 33, 36] Firstly, 3-5 nm seed gold nanoparticles were synthesized. Briefly, 1 mL, 34 mM sodium citrate was added into conical flask contained 100 mL $H_2O$ under vigorous stirring. Then added 1 mL, 24 mM $HAuCl_4$ into this mixture. After 1 min, 3 mL of ice-cold, fleshing prepared 0.1 M $NaBH_4$ solution was added with stirring. The solution turned brown immediately and gradually changed into wine red color. The solution was then stirred for 5 min and stored at 4℃ until needed.

Washing the commercial kitchen sponge by DI water and ethanol for three times and then dry in the oven. Cut the sponge into desired sizes. To grow vertical gold nanowires on the skeleton of bare sponge, the sponge was treated with 10 min air plasma to get fully hydrophilic skeleton. Then the sponge was soaked into APTMS (5 mM) ethanol solution for two hours. After washed by ethanol to remove redundant APTMS and completely dried by $N_2$ flow, the sponge was immersed into gold

seeds suspensions for another two hours to anchor Au seeds onto the skeleton of sponge. After Au seeds deposition, the sponge was washed by DI water and dried by $N_2$ flow. Then the sponge was put in v-AuNWs growth solution of ethanol/water (v/v=1:1.2), which contains $HAuCl_4$ (12 mM), ligand MBA (1.1 mM), L-AA (30 mM). After 5 min, the sample was washed by ethanol and dried by $N_2$ flow. The enokitake-like vertically aligned gold nanowires sponge was prepared.

***Fabrication and test of strain-insensitive v-AuNWs sponge conductors:*** In the first step, Ecoflex was infiltrated into v-AuNWs sponge with a dimension of 3 cm ×1 cm ×0.2 cm. Briefly, the mixture of Ecoflex curable silicone fluid A and B with a weight ratio of 1:1, was gently poured onto the as-prepared v-AuNWs sponge which two ends (each about 0.5 cm length) were exposed in air in the whole encapsulation process. Then the composite in procured Ecoflex was degassed in a desiccator for 2 hours, until no gas bubbles were observed on the surface of the mixture. Ecoflex encapsulation was completed by leaving the mixture in an oven at 60 ºC for 1 h. In the second step, using the aluminium foil cover two ends of the v-AuNWs sponge, and connecting with alligator clips of electrochemical workstation to characterize strain-dependent electrical properties of the v-AuNWs-sponge-Ecoflex composites.

***Fabrication of all-solid-state supercapacitors:*** Firstly, the PVA/$H_2SO_4$ gel electrolyte was prepared as previously reported.[37] 5 g $H_2SO_4$ was mixed with 50 mL DI water and then added 5 g PVA powder into the mixture. The whole mixture was heated to 80 °C under vigorous stirring until the solution became clear. Secondly, PANI was electrodeposited through an electropolymerization of aniline at potential of 0.8 V for 15 min in an aqueous solution of aniline (0.1 M) and $H_2SO_4$ (1 M) where KCl-saturated Ag/AgCl served as reference electrode and platinum wire as the counter electrode. Then, dipped the PANI/v-AuNWs sponge into PVA/$H_2SO_4$ gel electrolyte until the PANI/v-AuNWs sponges were saturated. Place two piece of PANI/v-AuNWs sponges onto two sputtered Au film with PET as substrates, respectively. Then put a piece filter paper with electrolytes saturated onto one of above PANI/v-AuNWs sponge electrode. Subsequently, both of PANI/AuNWs sponges were left in fume hood for several hours. After that, press two electrodes together and left at room temperature

for another several hours. Finally, all-solid-state PANI/v-AuNWs sponge based supercapacitor was fabricated (volume of the supercapacitor is 1cm×1cm×0.3cm). To fabricate a stretchable supercapacitor, one end of the of v-AuNWs sponge electrode was encapsulated with Ecoflex with the rest part impregnated with PVA/ $H_2SO_4$ gel electrolyte; a bare sponge was impregnated with PVA/ $H_2SO_4$ gel electrolyte was used as the separator. Then, they were assembled into a symmetrical sandwich-type structure, and left overnight until the electrolyte solidified into gels (**Figure S19**).

***Recyclable catalysis of 4-nitrophenol by v-AuNWs sponge:*** Typically, 15 mL of newly prepared 0.264 M sodium borohydride and 10 mL of 2.5 mM p-nitrophenol were mixed together in a beaker. The beaker was kept in a 45 ºC oven for 10 min, then a piece of v-AuNWs sponge was immersed into the solution for 15 min and 0.5 mL of the solution was extracted for further UV-vis absorption analysis at certain intervals. The above process was repeated 10 times to investigate the recycled efficiency of the gold nanowire sponge as the catalyst.

***Characterization:*** We used FEI Helios Nanolab 600/ FEI Quanta 250 FEG/ Hitachi S-4800 to obtain SEM images. Bending tests of supercapacitors and stretching tests of conductors were performed using motorized moving stages (THORLABS model LTS150/M) and electrical signals were recorded by the Parstat 2273 electrochemical system (Princeton Applied Research). We also used CHI660E Electrochemical Workstation for current record in the compression tests. The mechanical measurements were taken by a computer-based user interface and a force sensor (Force Gauge Model M7-2) and a motorized test stand (Mark-10). Pristine sponge and v-AuNWs sponge samples with a typical thickness of 5 mm were used for the mechanical testing. The motor speed was 0.01 mm/s, then we could obtain the stress-strain curves.

## Supporting Information

Supporting Information is available from the Online or from the author.

## Acknowledgements

This research was financially supported under Discovery Projects funding schemes (DP180101715 and DP200100624) and Linkage Projects scheme (LP160100521). This work was performed in part at the Melbourne Centre for Nanofabrication (MCN) in the Victorian Node of the Australian National Fabrication Facility (ANFF). Fenge Lin would like to thank the financial aid from Australian Government Research Training Program (RTP) Scholarship. We would like to thank A/Professor Yi Chen for providing experimental supports during the COVID-19 at the Monash Suzhou campus.

## Conflict of Interest

The authors declare no competing financial interest.

Received: (will be filled in by the editorial staff)

Accepted: (will be filled in by the editorial staff)

DOI: (will be filled in by the editorial staff)

## References


1. B. Zhu, S. Gong and W. Cheng, *Chem.Soc.Rev.*, 2019, **48**, 1668-1711.
2. S. Gong, L. W. Yap, B. Zhu and W. Cheng, *Adv. Mater.*, 2019, DOI: 10.1002/adma.201902278.
3. D. J. Lipomi, M. Vosgueritchian, B. C. Tee, S. L. Hellstrom, J. A. Lee, C. H. Fox and Z. Bao, *Nat. Nanotechnol.*, 2011, **6**, 788-792.
4. M. Vosgueritchian, D. J. Lipomi and Z. Bao, *Adv. Funct. Mater.*, 2012, **22**, 421-428.
5. R. C. Webb, A. P. Bonifas, A. Behnaz, Y. Zhang, K. J. Yu, H. Cheng, M. Shi, Z. Bian, Z. Liu, Y. S. Kim, W. H. Yeo, J. S. Park, J. Song, Y. Li, Y. Huang, A. M. Gorbach and J. A. Rogers, *Nat Mater*, 2013, **12**, 938-944.
6. A. Miyamoto, S. Lee, N. F. Cooray, S. Lee, M. Mori, N. Matsuhisa, H. Jin, L. Yoda, T. Yokota, A. Itoh, M. Sekino, H. Kawasaki, T. Ebihara, M. Amagai and T. Someya, *Nat. Nanotechnol.*, 2017, **12**, 907-913.
7. Y. Zhao, D. Dong, S. Gong, L. Brassart, Y. Wang, T. An and W. Cheng, *Adv. Electron. Mater.*, 2019, **5**, 1800462.
8. Y. Zhao, D. Dong, Y. Wang, S. Gong, T. An, L. W. Yap and W. Cheng, *ACS Appl. Mater. Interfaces*, 2018, **10**, 42612-42620.
9. Y. Wang, S. Gong, S. J. Wang, X. Yang, Y. Ling, L. W. Yap, D. Dong, G. P. Simon and W. Cheng, *ACS Nano*, 2018, **12**, 9742-9749.
10. S. Gong, L. W. Yap, B. Zhu, Q. Zhai, Y. Liu, Q. Lyu, K. Wang, M. Yang, Y. Ling, D. T. H. Lai, F. Marzbanrad and W. Cheng, *Adv. Mater.*, 2019, DOI: 10.1002/adma.201903789.
11. Y. Tang, S. Gong, Y. Chen, L. W. Yap and W. Cheng, *ACS Nano*, 2014, **8**, 5707-5714.
12. J. Ge, H. B. Yao, X. Wang, Y. D. Ye, J. L. Wang, Z. Y. Wu, J. W. Liu, F. J. Fan, H. L. Gao, C. L. Zhang and S. H. Yu, *Angew. Chem.*, 2013, **52**, 1968-1703.
13. Y. Yu, J. Zeng, C. Chen, Z. Xie, R. Guo, Z. Liu, X. Zhou, Y. Yang and Z. Zheng, *Adv. Mater.*, 2014, **26**, 810–815.
14. H. Chen, Z. Su, Y. Song, X. Cheng, X. Chen, B. Meng, Z. Song, D. Chen and H. Zhang, *Adv. Funct. Mater.*, 2017, **27**, 1604434.
15. Y. H. Wu, H. Z. Liu, S. Chen, X. C. Dong, P. P. Wang, S. Q. Liu, Y. Lin, Y. Wei and L. Liu, *ACS Appl. Mater. Interfaces*, 2017, **9**, 20098-20105.
16. Z. Niu, W. Zhou, X. Chen, J. Chen and S. Xie, *Adv. Mater.*, 2015, **27**, 6002-6008.
17. Y. Zhao, J. Liu, Y. Hu, H. Cheng, C. Hu, C. Jiang, L. Jiang, A. Cao and L. Qu, *Adv. Mater.*, 2013, **25**, 591-595.
18. H. W. Zhu, J. Ge, Y. C. Peng, H. Y. Zhao, L. A. Shi and S. H. Yu, *Nano Res.*, 2018, **11**, 1554-1562.
19. W. Chen, R. B. Rakhi, L. Hu, X. Xie, Y. Cui and H. N. Alshareef, *Nano Lett.*, 2011, **11**, 5165-5172.
20. X. Wu, Y. Han, X. Zhang, Z. Zhou and C. Lu, *Adv. Funct. Mater.*, 2016, **26**, 6246-6256.
21. S. Chun, A. Hong, Y. Choi, C. Ha and W. Park, *Nanoscale*, 2016, **8**, 9185-9192.
22. H. B. Yao, J. Ge, C. F. Wang, X. Wang, W. Hu, Z. J. Zheng, Y. Ni and S. H. Yu, *Adv. Mater.*, 2013, **25**, 6692–6698.
23. H. Zhang, N. Liu, Y. Shi, W. Liu, Y. Yue, S. Wang, Y. Ma, L. Wen, L. Li, F. Long, Z. Zou and Y. Gao, *ACS Appl. Mater. Interfaces*, 2016, **8**, 22374-22381.
24. Y. Tang, K. L. Yeo, Y. Chen, L. W. Yap, W. Xiong and W. Cheng, *J. Mater. Chem. A*, 2013, **1**, 6723-6726.
25. J. Y. Oh, D. Lee and S. H. Hong, *ACS Appl. Mater. Interfaces*, 2018, **10**, 21666-21671.
26. L. Xie, F. Su, L. Xie, X. Li, Z. Liu, Q. Kong, X. Guo, Y. Zhang, L. Wan, K. Li, C. Lv and C. Chen, *ChemSusChem*, 2015, **8**, 2917-2926.
27. Y. Wang, D. Kong, W. Shi, B. Liu, G. J. Sim, Q. Ge and H. Y. Yang, *Advanced Energy Materials*, 2016, **6**, 1601057.
28. S. Gong, Y. Wang, L. W. Yap, Y. Ling, Y. Zhao, D. Dong, Q. Shi, Y. Liu, H. Uddin and W. Cheng, *Nanoscale Horizons*, 2018, **3**, 640-647.
29. S. Gong, L. W. Yap, B. Zhu, Q. Zhai, Y. Liu, Q. Lyu, K. Wang, M. Yang, Y. Ling, D. T. H. Lai, F. Marzbanrad and W. Cheng, *Adv. Mater.*, 2019, DOI: 10.1002/adma.201903789, 1903789.
30. T. An, Y. Ling, S. Gong, B. Zhu, Y. Zhao, D. Dong, L. W. Yap, Y. Wang and W. Cheng, *Adv. Mater. Technol.*, 2018, DOI: 10.1002/admt.201800473.
31. T. An, B. Zhu, Y. Ling, S. Gong and W. Cheng, *J. Mater. Chem. A*, 2019, **7**, 14233-14238.

32. Q. Zhai, Y. Liu, R. Wang, Y. Wang, Q. Lyu, S. Gong, J. Wang, G. P. Simon and W. Cheng, *Advanced Energy Materials*, 2019, DOI: 10.1002/aenm.201903512.
33. Y. Wang, S. Gong, D. Gomez, Y. Ling, L. W. Yap, G. P. Simon and W. Cheng, *ACS Nano*, 2018, **12**, 8717-8722.
34. Q. Zhai, Y. Wang, S. Gong, Y. Ling, L. W. Yap, Y. Liu, J. Wang, G. P. Simon and W. Cheng, *Anal Chem*, 2018, **90**, 13498-13505.
35. K. Wang, F. Lin, D. T. H. Lai, S. Gong, B. Kibret, M. A. Ali, M. R. Yuce and W. Cheng, *Nanoscale*, 2021, **13**, 3957-3966.
36. B. Zhu, S. Gong, F. Lin, Y. Wang, Y. Ling, T. An and W. Cheng, *Adv. Electron. Mater.*, 2019, **5**, 1800509.
37. Z. Niu, H. Dong, B. Zhu, J. Li, H. H. Hng, W. Zhou, X. Chen and S. Xie, *Adv. Mater.*, 2013, **25**, 1058–1064.

**FIGURE**

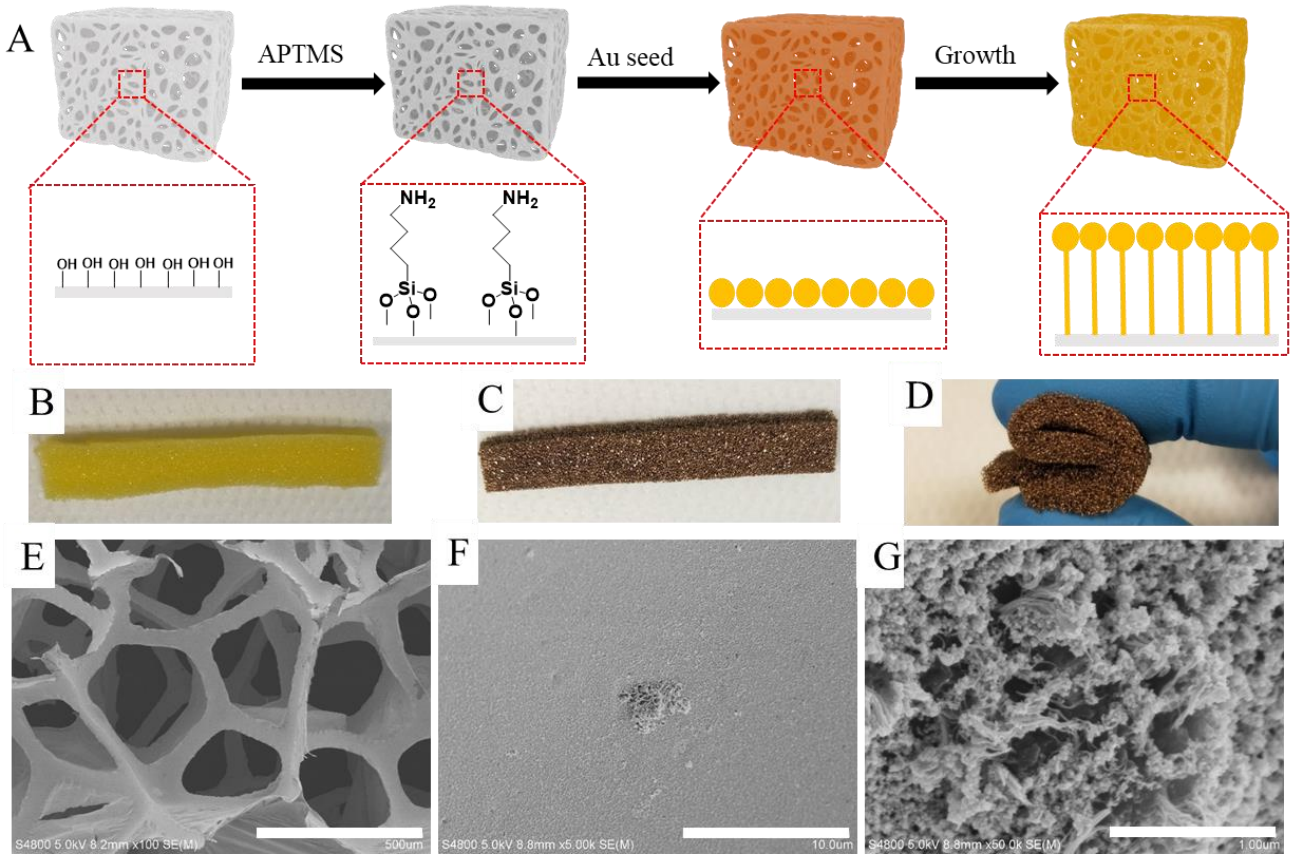


**Figure 1.** (A) Schematic diagram of synthesizing v-AuNWs sponge. (B, C) Photographs of PU sponge before (B) and after (C) v-AuNWs grow. (D) Photograph of v-AuNWs sponge be folded. (E-G) SEM images of v-AuNWs sponge, scale bar is scale bar is 500 μm, 5 μm and 500 nm respectively.

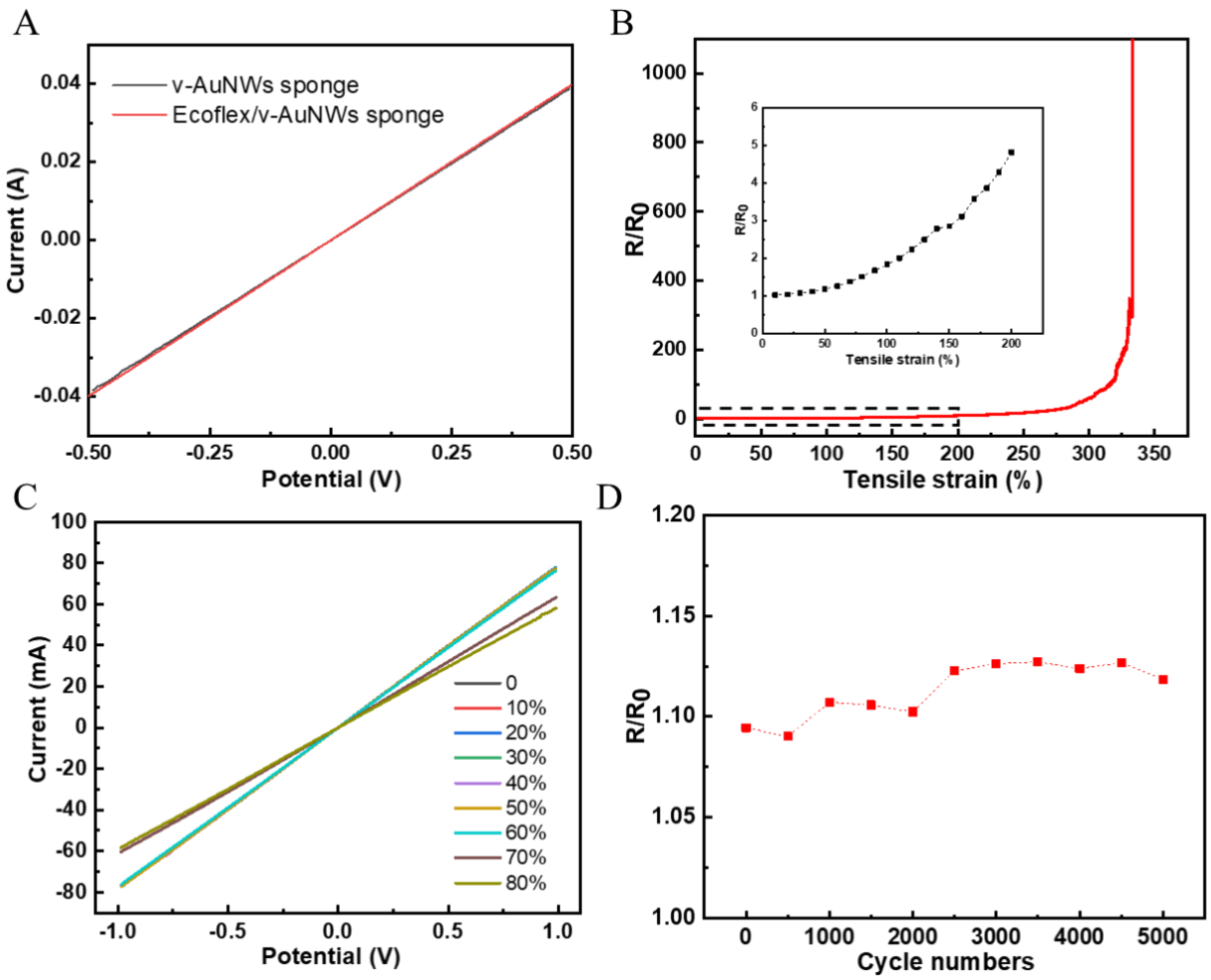


**Figure 2.** (A) I-V curves of v-AuNWs before and after Ecoflex embedded. (B) Stretchability of v-AuNWs sponge/ Ecoflex conductor (the insert one is the magnification of relative resistance change of v-AuNWs sponge/ Ecoflex conductor under 200%). (C) I−V curves of the v-AuNWs sponge/ Ecoflex conductor at different stretching strain levels. (D) Durability of the v-AuNWs sponge/ Ecoflex conductor at 30% stretching strain.

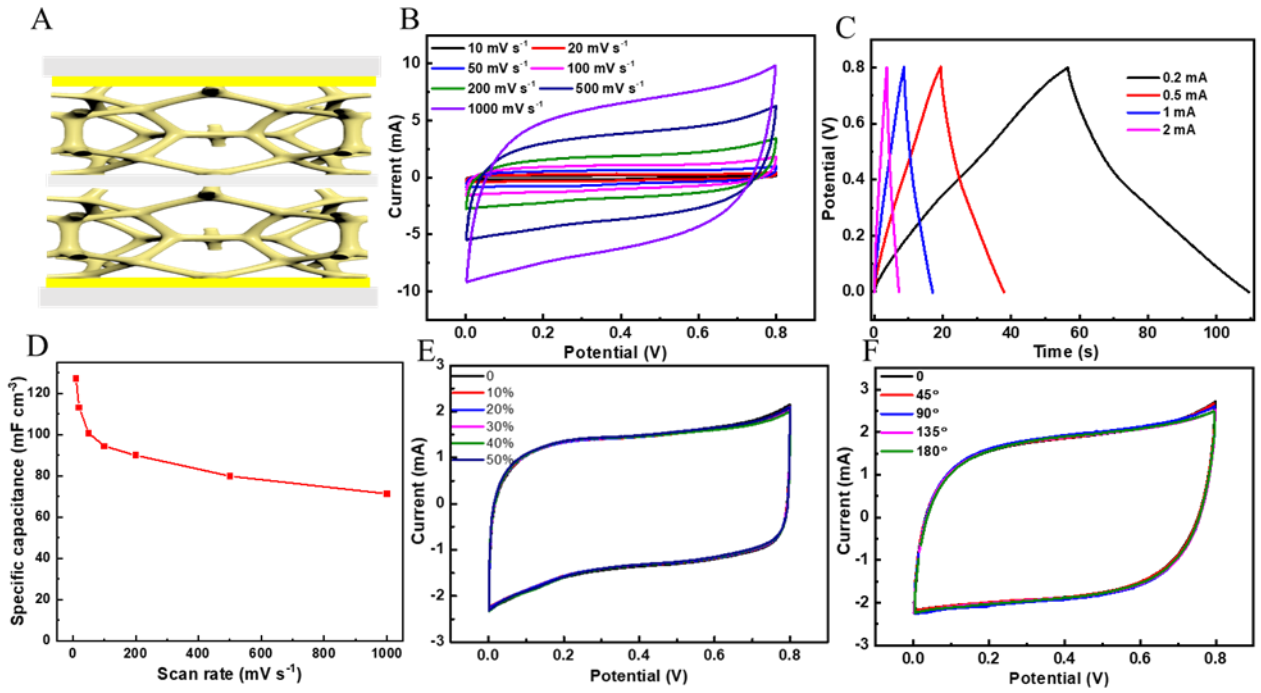


**Figure 3**. (A) Schematic illustration of v-AuNWs/PANI sponge supercapacitor. (B) CV curves of v-AuNWs/PANI sponge based supercapacitors at various scan rates. (C) GCD curves v-AuNWs/PANI sponge based supercapacitor under various current. (D) Volume specific capacitances at different scan rates. (E) CV curves at 200 mV $s^{-1}$ under different compressing strains from 0 to 50%. (F) CV curves at 200 mV $s^{-1}$ under different bending degrees from 0 to 180º.

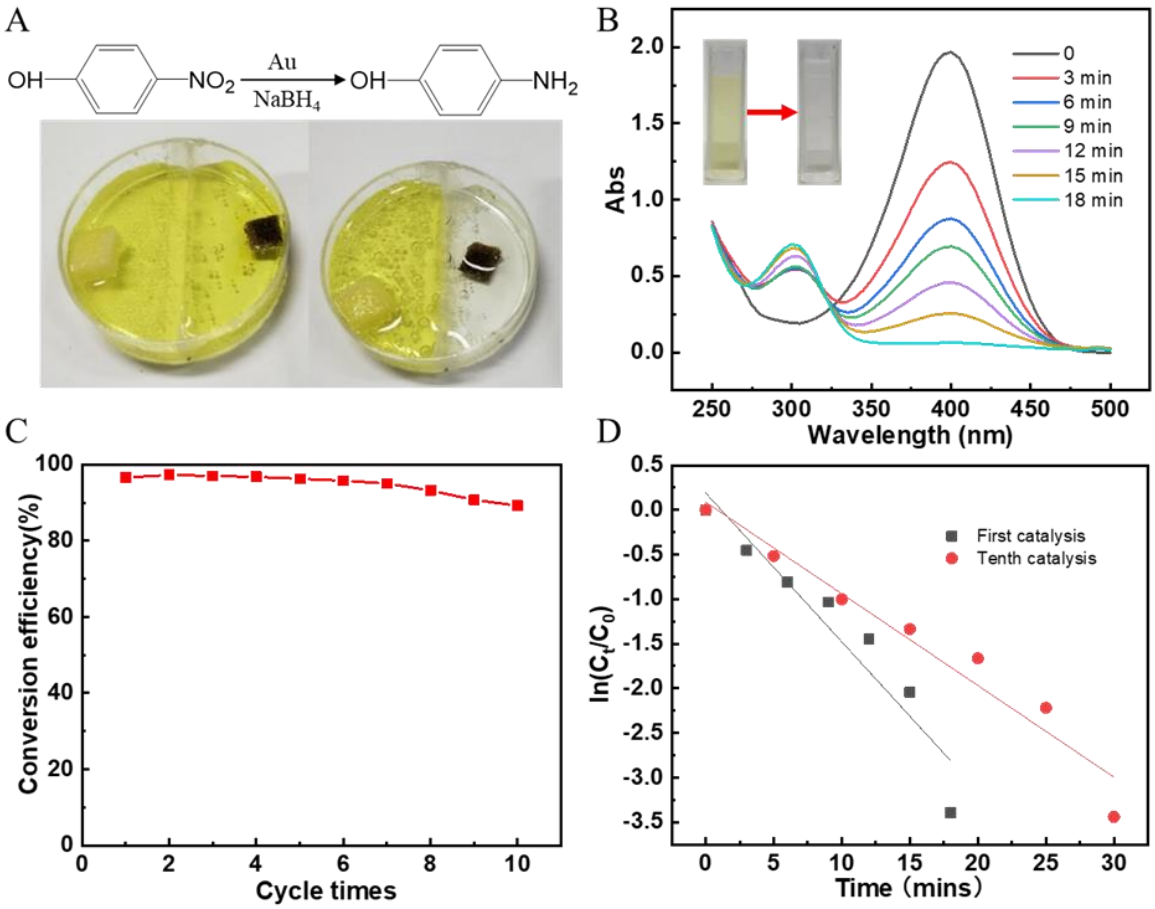


**Figure 4.** (A)Photographic illustration of the reduction of p-nitrophenol by $NaBH_4$ under catalysis of V-AuNWs sponge. (B) The reduction of p-nitrophenol in aqueous solution recorded at several intervals V-AuNWs sponge as a catalyst. (C) The reusability of the V-AuNWs sponge as a catalyst for the reduction of 4-nitrophenol by $NaBH_4$. (D) The relationship between $\ln(C_t/C_0)$ and reaction time (t) of different catalysis times.